Acta Cryst. (1988). B44, 89–96

Structure of β-Uranium

BY A. C. LAWSON AND C. E. OLSEN

Materials Science and Technology Division, Los Alamos National Laboratory, Los Alamos, New Mexico 87545, *USA*

AND J. W. RICHARDSON JR, M. H. MUELLER AND G. H. LANDER*

Intense Pulsed Neutron Source Division, Argonne National Laboratory, Argonne, Illinois 60439, *USA*

(*Received* 24 *March* 1987; *accepted* 22 *September* 1987)

Abstract

The β-structure of uranium metal is stable between 935 and 1045 K. Profile refinements of time-of-flight neutron diffraction data show that the space group of this structure is $P4_2/mnm$. This finding ends a long controversy dating back to the 1950's. The details of these experiments and analyses, which include the separation of the crystalline scattering of the powdered uranium from the diffuse scattering of a fused silica container and a comparison of results from powder and polycrystalline rod samples, are reported.

Introduction

The element uranium has three allotropes. Up to 935 K the orthorhombic α-form (*Cmcm*, No. 63) exists with four atoms per unit cell. From 935 to 1045 K the β-form exists. This is known to be tetragonal with 30 atoms per unit cell but the precise space group has not been assigned despite many efforts between 1948 and 1971 to determine it. At 1045 K uranium transforms to the γ-form which is simple b.c.c. with two atoms per unit cell. It melts at 1405 K. Donohue (1974) gives a very thorough survey of the state of the controversy over the β-uranium structure; to our knowledge no new work has been done since 1974. The three space groups that have been suggested for β-uranium are $P4_2nm$ (No. 102), $P\bar{4}n2$ (No. 118), both of which are noncentrosymmetric, and $P4_2/mnm$ (No. 136), which is centrosymmetric. An earlier shorter summary was given by Donohue & Einspahr (1971).

Our own interest in uranium is a consequence of recent developments in the low-temperature α-phase. As summarized recently by Smith & Lander (1984), at low temperatures (<43 K) the α-phase exhibits at least one, and possibly two, charge-density-wave distortions. The great structural complexity of the allotropes of the actinide metals (Donohue, 1974) is now generally recognized to be due to the presence of *f* bonding (*i.e.*, participation of the 5*f* electrons in the bonding process). A consequence of this is that when one reaches Am, in which the 5*f* electrons are localized, the structural forms are simple (namely, double-hexagonal close-packed and cubic close-packed). Although band-structure calculations have not yet solved the details of these structures (Brooks, Johansson & Skriver, 1984), progress has been made on understanding the role of 5*f* electrons.

The determination of the structure of β-uranium is necessarily beset with difficulty. In the first place, no single crystals of pure β-uranium have yet been obtained, so that it is necessary to use high-temperature powder diffraction techniques. Single crystals of β-uranium alloys can be prepared and quenched to room temperature, and such crystals stabilized with 1·4 at.% Cr have been used in previous investigations, but it is not known whether these alloys have the same structure as the pure element in the β-region. In view of the extent of the controversy over previous results, it seems desirable to study the pure element.

The use of X-rays for obtaining powder diffraction patterns at high temperatures is intrinsically complicated by three properties of uranium: its high reactivity, its radioactivity and its high absorption cross-section for X-rays. Uranium must be encapsulated to prevent oxidation and to prevent the spread of radioactive contamination in the case of an accident. Because of the reactivity, any imperfections in the containment are guaranteed to produce surface contamination of UO and UO_2 which, because of the absorption, will further obscure the diffraction pattern even if the volume fraction of contaminant is small.

For all these reasons we have brought the technique of neutron powder diffraction to bear on the β-uranium problem. Absorption is very small with neutrons, and most of the problems encountered with X-ray diffraction are much less severe. We were also able to take advantage of the Rietveld method (Rietveld, 1969; Von Dreele, Jorgensen & Windsor, 1982; Jorgensen & Rotella, 1982) and the high resolution available with a powder diffractometer on a pulsed neutron source.

* Present address: Transuranium Institute, Euratom, Postfach 2340, D-7500 Karlsruhe, Federal Republic of Germany.

0108-7681/88/020089-08$03.00

Experimental

The experiments were performed on the General Purpose Powder Diffractometer (GPPD) at the Intense Pulsed Neutron Source, Argonne National Laboratory. This diffractometer has a resolution of 0·3% over all d spacings from 0·4 to 3·0 Å at a scattering angle of 150°. The neutron wavelength is determined by the time of flight over the source-to-sample length of 20 m and sample-to-detector length of 1·5 m. A more complete description of the instrument is given by Jorgensen & Faber (1982).

In addition to the experimental problems which we have already mentioned, there is also the well-known problem of grain growth that takes place at elevated temperatures in uranium. A consequence of this phenomenon is that one must be prepared for the development of preferred orientation (or texture) in ostensibly random powder patterns at high temperature. Such an effect might, of course, seriously influence any attempt to refine the structural parameters of the β-phase. [An important technological consequence of this grain growth, especially in the γ-phase, is that the subsequent anisotropic thermal expansion in the α-phase (Chiotti, Klepfer & White, 1959) gives rise to enormous intergranular stresses. This discovery in the 1950's contributed to the decision to abandon uranium metal as a nuclear fuel.]

Our first experiments were performed on a bundle of high-purity polycrystalline rods (height = 50 mm, diameter = 1 mm), which were supported in vacuum by a vanadium tube. In order to reduce as much as possible any intrinsic preferred orientation, the rods were heat treated in the β-phase and also in the γ-phase regions. In addition, the sample was rotated at 1 r.p.m. to minimize the consequences of any remaining preferred orientation and grain-size effects. The relative intensities of several low-index reflections were used to judge the efficacy of these procedures. Patterns were obtained for the α- and β-phases, and the β-phase patterns were refined in the three possible space groups for β-uranium as discussed by Donohue. Weighted-profile residual-agreement-factor (R_{wp}) values of 5·55, 5·66 and 5·49% were obtained for space groups $P4_2nm$ (No. 102), $P\bar{4}n2$ (No. 118) and $P4_2/mnm$ (No. 136), respectively. Although the R_{wp}'s are nearly the same, there are more parameters refined in the lower symmetry space groups, so that there is some indication that No. 136 ($P4_2/mnm$) is the correct space group. Unfortunately, failure of the furnace necessitated a premature termination of these experiments, and because of poor counting statistics the agreement factors were higher than anticipated. We also suspected that preferred orientation might still be a problem.

This problem, as well as other grain-size-related problems, can of course be eliminated better if uranium *powder* is used, although then we can no longer use a metal container, because of the increased reactivity due to the much larger surface area. Approximately 30 g of uranium metal powder was prepared by dehydriding UH_3 which had previously been prepared from high-purity polycrystalline metal. The dehydriding was carried out for 8 h under vacuum at 1073 K in a fused silica tube which had been coated internally with a thin layer of pyrolytic graphite in order to reduce the reactivity of the silica. Upon completion of the dehydriding the tube was backfilled with helium gas and sealed. The silica tubes were suspended in a furnace with vanadium foil heating elements, and in a second series of diffraction experiments we obtained patterns for the α-, β- and γ-phases. The temperature profile of this furnace was carefully determined, and the accuracy of the reported temperatures is estimated to be ±5 K. No visible reaction was observed between the silica and the uranium powder up to 1273 K, but the presence of a small amount of UO and UO_2 was detected in the diffraction patterns of the γ-phase, indicating that some reaction had occurred. The quantity of oxide is estimated to be no more than a few percent, which is not enough to interfere with the analysis of the data; in any case, the impurity contribution is certainly less for the β-phase patterns which were taken at lower temperatures. Even with the powder samples, we observed some grain growth in cooling from the γ- to α-phase at the end of the experiment. This could be observed directly at the time of the experiment by comparing intensities scattered into different detectors located on opposite sides of the incident beam, but at the same scattering angle. For this reason only the data taken on heating between 298 and 1073 K will be discussed in this paper.

Results and analysis

We show in Fig. 1 the pattern of β-uranium taken at 955 K from the powder in the silica tube.* Peaks in the β-phase extend from d spacings of ~0·4 to 2·87 Å. Peaks at larger values of d are not visible at $2\theta = 150°$ but are seen in the $2\theta = 90°$ detectors. Only the 150° data were used in the present refinement. The 'tick' marks just below the diffraction pattern are the possible d values for the β-phase. The complexity of the β-phase is indicated by the density of the diffraction lines below ~1·2 Å. A dominant feature of the difference pattern in Fig. 1 is the very large undulating background below $d = 1·5$ Å which comes from the silica tube. Since it is the data below $d \simeq 2$ Å that will give the most stringent test for the various space groups, this is unfortunate. However, a method has been developed at Argonne by

* A list of numerical values corresponding to the data in Figs. 1 and 2 has been deposited with the British Library Document Supply Centre as Supplementary Publication No. SUP 44463 (12 pp.). Copies may be obtained through The Executive Secretary, International Union of Crystallography, 5 Abbey Square, Chester CH1 2HU, England.

Richardson & Faber (1986) for handling this component in time-of-flight diffraction patterns from crystalline materials. The method is based on the fact that the diffuse intensity from amorphous materials (here from the silica) varies only slowly as a function of the scattering vector Q ($\equiv 2\pi/d$), whereas crystalline materials exhibit sharp Bragg peaks, and hence the amorphous component may be separated out by 'Fourier filtering.' The result of this filtering, together with the consequent refinement by the Rietveld method to fit the complete profile, is shown in Fig. 2. Note that in the first frame (low d) the difference pattern is quite flat, in contrast to that in Fig. 1. The diffuse component

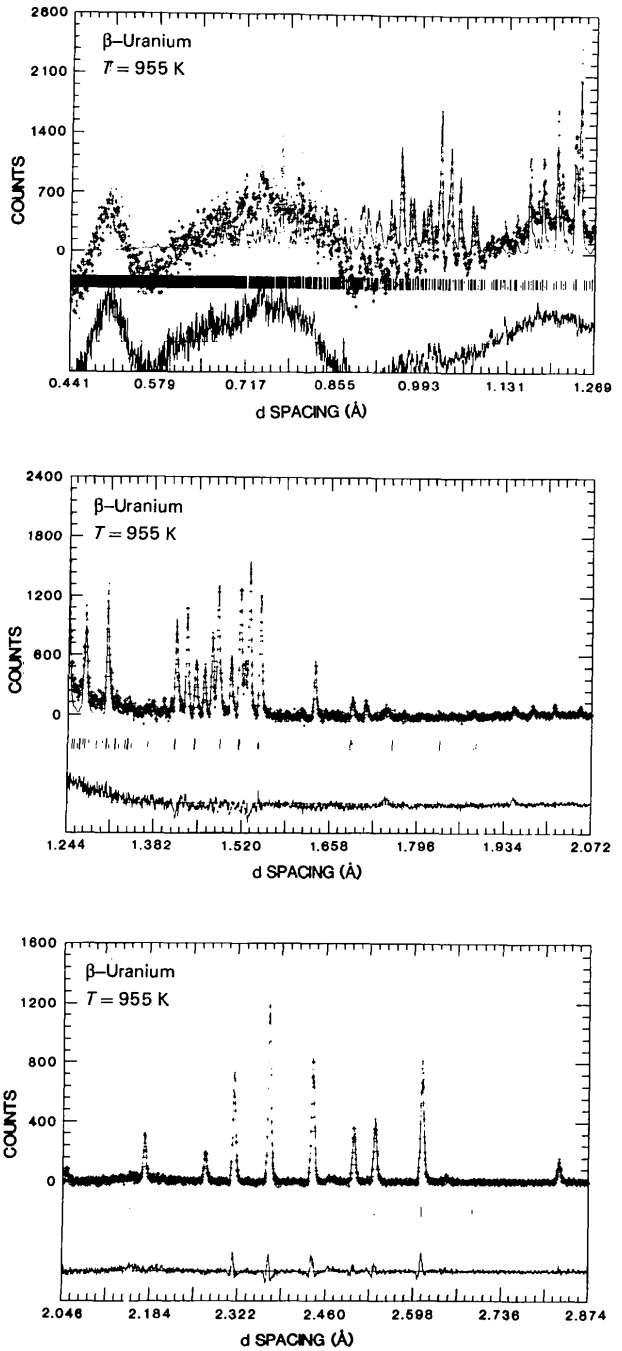

Fig. 1. Neutron diffraction patterns over the range $0{\cdot}4 < d < 2{\cdot}87$ Å for β-uranium at 955 K. Crosses are data points and the solid line is a best fit without any attempt to account for diffuse scattering from the quartz container. The tick marks below the figure are the allowed d values and the lower curve is a difference (observed minus calculated) plot.

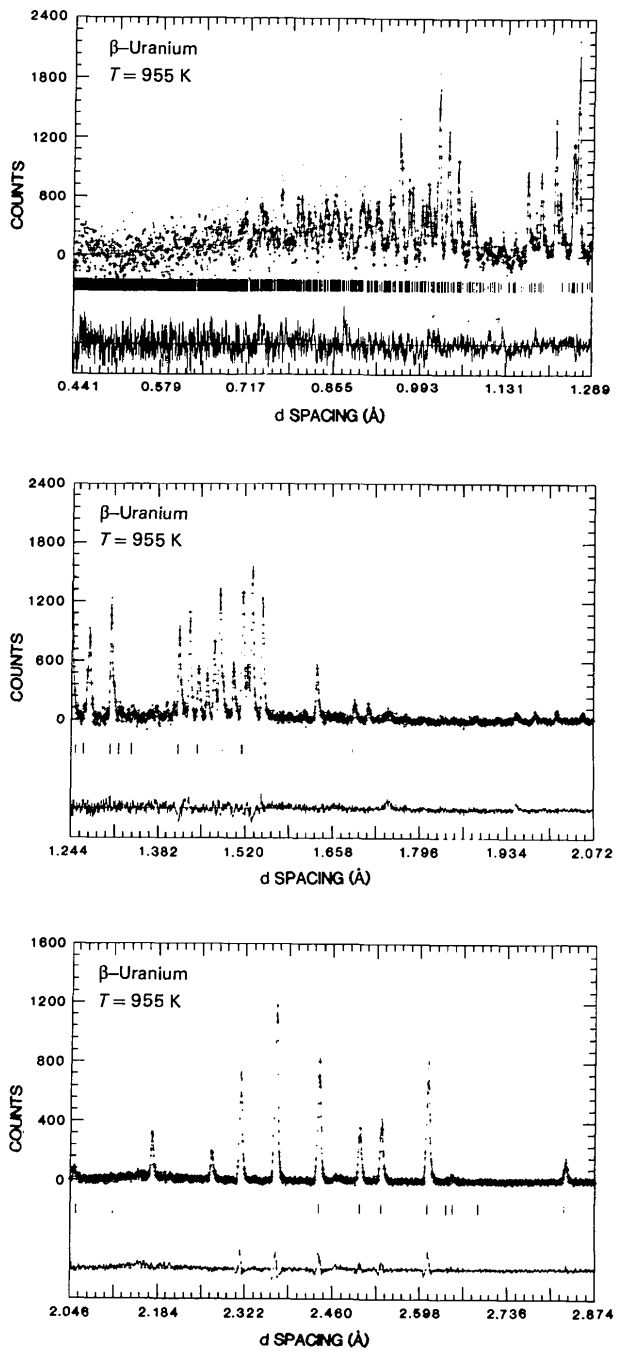

Fig. 2. As Fig. 1, but with Fourier filtering to remove the diffuse component.

from the silica, as separated by the filtering technique, is plotted as a function of Q, which is the more conventional way, in Fig. 3. Overall, the pattern is in agreement with those measured for room-temperature amorphous SiO_2 (Arai, 1984). The small differences around 8–10 $Å^{-1}$ between the silica pattern of Fig. 2 and those measured for room temperature silica probably represent real differences induced by temperature. The filtered data were refined using the Rietveld technique. Crystallographic, scale-factor and background parameters were refined; the profile parameters were those obtained for silicon powder in a room-temperature calibration experiment, and absorption and extinction factors were fixed at zero. Subsequent refinements of profile, absorption and extinction parameters resulted in negligible shifts, thus justifying the original values.

The refinement of the uranium patterns gives the lattice and thermal parameters, as well as the atomic coordinates. We present some of these data in Table 1 in order to show the consistency of our results. Our values for the lattice constants are in agreement with, but of higher precision than, those of Chiotti *et al.* (1959), and the variation of the y parameter in the α-phase, which is the only structural parameter to be refined in this phase, is in good agreement with that reported by Mueller, Hitterman & Knott (1962). The atomic volume can be derived from the lattice constant results, and it is plotted *versus* temperature in Fig. 4. Values for temperatures below 300 K are taken from

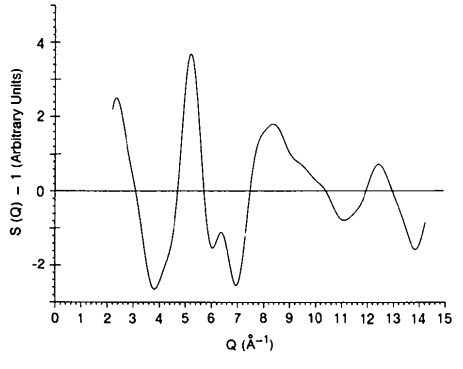

Fig. 3. The diffuse component (from the quartz tube) as separated from the crystalline diffraction pattern (Fig. 2) and plotted as a function of $Q(=2\pi/d)$. The pattern cuts off at $Q = 2$ $Å^{-1}$ because we have no d values longer than ~3 Å in the $2\theta = 150°$ detectors.

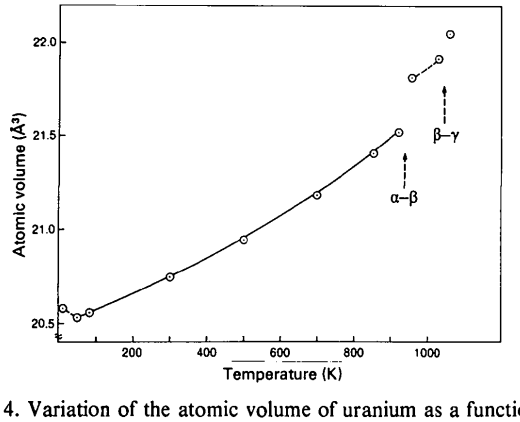

Fig. 4. Variation of the atomic volume of uranium as a function of temperature. The solid line is the fit to the thermal expansion coefficient as discussed in the text. Note the volume discontinuities associated with the phase transitions.

Table 1. *Lattice parameters as a function of temperature for uranium*

Unless otherwise noted, standard deviations are ±1 on all least significant figures; except a and c for β-uranium, where the numbers are ±2. The values in square brackets are those recommended at room temperature by Donohue (1974).

T(K)	Phase	a (Å)	b (Å)	c (Å)	At. vol. (Å³)	γ ($\Delta V/V$) (10^{-6} K^{-1})
298	α	2·8539	5·8678	4·9554	20·746	
		[2·8538]	[5·8680]	[4·9557]		48
498	α	2·8685	5·8675	4·9774	20·944	
						57
698	α	2·8876	5·8588	5·0085	21·183	
						68
850	α	2·9066	5·8443	5·0397	21·402	
						81
919	α	2·9178	5·8340	5·0570	21·521	
						376 (3)
955	β	10·7589		5·6531	21·812	
						62 (2)
1030	β	10·7766		5·6609	21·914	
						206 (3)
1060	γ	3·5335			22·050	

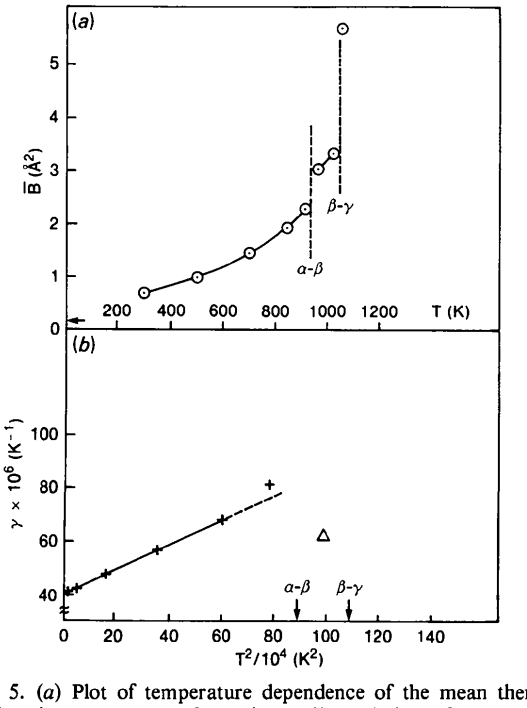

Fig. 5. (*a*) Plot of temperature dependence of the mean thermal vibration parameter of uranium. (*b*) Variation of the volume expansion coefficient γ as a function of T^2. (Note that this γ should not be confused with the high-temperature γ-phase of uranium.)

Barrett, Mueller & Hitterman (1963). The volume thermal expansion coefficient γ between room temperature and 498 K is 48×10^{-6} K^{-1}, slightly larger, as expected, than the value below room temperature given by Barrett *et al.* (Unfortunately convention requires us to use the symbol γ for both the high-temperature b.c.c. phase and for the thermal expansion coefficient; the meaning should be clear from the context.) An analysis of the thermal expansion coefficient (Fig. 5*b*) shows that it follows the expected temperature dependence $\gamma = A + BT^2$ with $A = (4{\cdot}1 \pm 0{\cdot}2) \times 10^{-5}$ K^{-1} and $B = (4{\cdot}6 \pm 0{\cdot}2) \times 10^{-11}$ K^{-3} for $50 < T < 850$ K. Just before the $\alpha \rightarrow \beta$ transition the thermal expansion increases and a sudden discontinuity occurs in the volume at this phase transition. There is a smaller but significant discontinuity at the $\beta \rightarrow \gamma$ transition.

We have also determined an overall, isotropic thermal parameter $\bar{B}$ which is plotted *versus* temperature in Fig. 5(*a*). The thermal parameters are known to be anisotropic in the α-phase (Lander & Mueller, 1970), and we find agreement that the vibration along the *a* axis is the largest. The zero-point thermal motion corresponds to a Debye temperature Θ of ~150 K, and $\bar{B}$ then rises almost linearly, which is expected for $T > 3\Theta$, until just before the $\alpha \rightarrow \beta$ transition. The values of $\bar{B}$ in the β-phase are considerably larger than those in the α-phase, and a further large jump in $\bar{B}$ occurs at the transformation to the γ-phase. Mueller *et al.* (1962) also reported B values up to 898 K but, because they looked primarily at (0*k*0) reflections, they really determined B_{22}, and this is somewhat lower than $\bar{B}$ because of the anisotropy discussed earlier.

Structure of the β-phase

Controversy over the structure of the β-phase is possible because the observed reflections are allowed by three possible space groups, as pointed out by Donohue: $P4_2nm$ (No. 102), $P\bar{4}n2$ (No. 118) and $P4_2/mnm$ (No. 136). Of these, only the last (No. 136) is centrosymmetric. The two space groups of lesser symmetry are subgroups of No. 136 but not of each other, and each of the three possible space groups is a supergroup of the orthorhombic space group *Pnn*2 (No. 34). Because the origin of space group No. 118 is not the same as the other two, we refined the β-uranium data in the orthorhombic space group and used extra constraints on the coordinates and components of the thermal tensor to reproduce the symmetry elements of the three candidate space groups. For the non-centrosymmetric space groups, instabilities in the refinements were avoided by choosing starting values for the atomic coordinates obtained by slightly displacing the atoms from their positions in the centrosymmetric space group. This procedure allows us to describe all the groups with the same notation, and we have reproduced such a description (Donohue's Table 92-5) as Table 2.

Table 2. *Possible descriptions of the β-uranium unit cell, following Donohue* (1974)

Atom numbers I, *etc.*, refer to Table 3.

Space group $P4_2nm$ (No. 102)
I Two atoms in 2*a*
$(00\frac{1}{2})$ $(\frac{1}{2}\frac{1}{2}0)$
II, IIIa, IIIb 12 atoms in three sets of 4*c*
(xxz) $(\bar{x}\bar{x}z)$ $(\frac{1}{2}+x, \frac{1}{2}-x, \frac{1}{2}+z)$ $(\frac{1}{2}-x, \frac{1}{2}+x, \frac{1}{2}+z)$
IV, V 16 atoms in two sets of 8*d*
(xyz) $(\bar{x}\bar{y}z)$ $(\frac{1}{2}+x, \frac{1}{2}-y, \frac{1}{2}+z)$ $(\frac{1}{2}-x, \frac{1}{2}+y, \frac{1}{2}+z)$
(yxz) $(\bar{y}\bar{x}z)$ $(\frac{1}{2}+y, \frac{1}{2}-x, \frac{1}{2}+z)$ $(\frac{1}{2}-y, \frac{1}{2}+x, \frac{1}{2}+z)$
Six atom types, 12 positional parameters, 27 anisotropic B_{ij}

Space group $P\bar{4}n2$ (No. 118) [origin moved to $(0\frac{1}{4}\frac{1}{4})$]
I Two atoms in 2*d*
$(00\frac{1}{2})$ $(\frac{1}{2}\frac{1}{2}0)$
II Four atoms in 4*g*
$(xx0)$ $(\bar{x}\bar{x}0)$ $(\frac{1}{2}-x, \frac{1}{2}+x, \frac{1}{2})$ $(\frac{1}{2}+x, \frac{1}{2}-x, \frac{1}{2})$
IIIa, IIIb, IV, V 24 atoms in three sets of 8*i*
(xyz) $(\bar{x}\bar{y}z)$ $(\frac{1}{2}-x, \frac{1}{2}+y, \frac{1}{2}+z)$ $(\frac{1}{2}+x, \frac{1}{2}-y, \frac{1}{2}+z)$
$(yx\bar{z})$ $(\bar{y}x\bar{z})$ $(\frac{1}{2}-y, \frac{1}{2}+x, \frac{1}{2}-z)$ $(\frac{1}{2}+y, \frac{1}{2}-x, \frac{1}{2}-z)$
Five atom types, 10 positional parameters, 25 anisotropic B_{ij}

Space group $P4_2/mnm$ (No. 136)
I Two atoms in 2*b*
$(00\frac{1}{2})$ $(\frac{1}{2}\frac{1}{2}0)$
II Four atoms in 4*f*
$(xx0)$ $(\frac{1}{2}+x, \frac{1}{2}-x, \frac{1}{2})$ + center of inversion
IIIa, IIIb Eight atoms in 8*j*
(xxz) $(\bar{x}\bar{x}z)$ $(\frac{1}{2}+x, \frac{1}{2}-x, \frac{1}{2}+z)$ $(\frac{1}{2}-x, \frac{1}{2}+x, \frac{1}{2}+z)$ + center of inversion
IV, V 16 atoms in two sets of 8*i*
$(xy0)$ $(yx0)$ $(\frac{1}{2}+x, \frac{1}{2}-y, \frac{1}{2})$ $(\frac{1}{2}+y, \frac{1}{2}-x, \frac{1}{2})$ + center of inversion
Five atom types, seven positional parameters, 18 anisotropic B_{ij}

Additional information is given on the number of refinable parameters. The key questions concern the *z* parameter of atoms II, IV and V (see Table 3 for these identifications), whether atoms IIIa and IIIb in No. 102 are related by a simple inversion, and whether for atom IIIa in No. 118 the *x* and *y* coordinates are equal. As emphasized by Donohue, these questions are subtle ones, and the answers can be given only by refinements of high-quality data.

The results of this work and of previous refinements are presented in Table 3. Rather than tabulate all previous values [which has already been done by Donohue (1974)] we have given the range into which the reported values fall. It should be noted that these ranges also include results at room temperature for chromium-stabilized β-uranium. Excluding these does not significantly change the ranges. Standard deviations were not reported for the previous refinements so we are unable to calculate a weighted mean. In the case of No. 118 only one previous refinement was reported.

For the present work we have given the values from the 955 K experiment. In all cases the results for the 955 and 1030 K runs are within each other's standard deviations. This observation appears to exclude the occurrence of a structural transformation within the β-phase, as might be inferred from the work of Duwez (1953). The refinements which we have reported have used anisotropic thermal parameters. In all space groups a number of refinements were performed using different starting parameters. The final values were in all cases within two standard deviations of the values in Table 3. The first and most important observation to be made from the 'this work' entries in Table 3 is that all

Table 3. *Comparison of least-squares results for uranium powder at* 955 K *using three space groups*

In No. 102 origin moved to place atom I at $x=y=0$, $z=\frac{1}{4}$. Values in square brackets are fixed by symmetry.

		$P4_2nm$ (No. 102)		$P\bar{4}n2$ (No. 118)		$P4_2/mnm$ (No. 136)	
		Previous	This work	Previous	This work	Previous	This work
I	$x=y$	[0]	[0]	[0]	[0]	[0]	[0]
	z	[0·5]	[0·5]	[0·5]	[0·5]	[0·5]	[0·5]
II	x	0·107→0·110	0·1029 (5)	0·100	0·1029 (4)	0·098→0·103	0·1030 (4)
	z	−0·014→0·070	−0·0072 (49)	[0]	[0]	[0]	[0]
IIIa	x	0·290→0·320	0·3194 (11)	0·313	0·3214 (10)	0·316→0·321	0·3188 (2)
	y	x	x	0·323	0·3160 (9)	x	x
	z	0·769→0·840	0·7458 (52)	0·725	0·7442 (16)	0·720→0·730	0·7444 (14)
IIIb	x	0·671→0·690	0·6827 (8)	Inverse of		Inverse of	
	y	x	x	IIIa		IIIa	
	z	0·294→0·340	0·2539 (49)	coordinates		coordinates	
IV	x	0·547→0·563	0·5622 (5)	0·557	0·5622 (4)	0·556→0·561	0·5622 (4)
	y	0·220→0·240	0·2357 (5)	0·228	0·2343 (4)	0·214→0·235	0·2343 (5)
	z	0·052→0·090	−0·0144 (44)	0·043	−0·0037 (21)	[0]	[0]
V	x	0·367→0·380	0·3652 (4)	0·368	0·3652 (4)	0·367→0·370	0·3655 (4)
	y	0·040→0·045	0·0402 (5)	0·041	0·0399 (4)	0·038→0·046	0·0391 (4)
	z	−0·026→0·040	−0·0033 (48)	−0·017	0·0077 (29)	[0]	[0]
R_{F^2} (%)			11·04		11·50		12·22
R_{wp} (%)			2·05		2·05		2·07
R_{exp} (%)			1·63		1·63		1·63

Table 4. *Anisotropic displacement parameters* ($\times 10^3$) *obtained from data using space group* $P4_2/mnm$ *at* 955 K

The displacement factors have the form $\exp[-\frac{1}{4}(B_{11}h^2a^{*2}+\ldots+2B_{23}klb^*c^*)]$.

	B_{11}	B_{22}	B_{33}	B_{12}	B_{13}	B_{23}
I	3·2 (2)	3·2	3·1 (5)	0·0 (3)	[0]	[0]
II	3·3 (2)	3·3	3·4 (3)	0·9 (2)	[0]	[0]
III	3·1 (1)	3·1	2·5 (1)	0·1 (1)	−0·1 (1)	−0·1
IV	3·1 (2)	3·0 (2)	4·1 (2)	0·2 (1)	[0]	[0]
V	2·5 (2)	3·4 (2)	3·8 (3)	−0·2 (1)	[0]	[0]

Table 5. *Least-squares results from refinements of β-uranium powder in* $P4_2/mnm$ *(No.* 136*) with and without Fourier filtering, at two temperatures and from β-uranium rods*

In the uncorrected data R_{F^2} is strongly influenced by the poor background fit (see Fig. 1), whereas R_{wp} is not affected.

		Uncorrected powder (955 K)	Corrected powder (955 K)	Corrected powder (1030 K)	Rods (973 K)*
I	$x=y$	[0]	[0]	[0]	[0]
	z	[0·5]	[0·5]	[0·5]	[0·5]
	$\bar{B}$	1·5 (2)	3·29 (15)	3·43	2·31 (12)
II	$x=y$	0·1013 (9)	0·1030 (4)	0·1026 (9)	0·1041 (4)
	z	[0]	[0]	[0]	[0]
	$\bar{B}$	5·0 (3)	3·76 (12)	3·52	2·36 (8)
III	$x=y$	0·3200 (4)	0·3188 (2)	0·3187 (5)	0·3188 (2)
	z	0·7542 (26)	0·7444 (14)	0·7482 (30)	0·7421 (8)
	$\bar{B}$	2·9 (1)	3·00 (5)	3·01	2·11 (5)
IV	x	0·5621 (9)	0·5622 (4)	0·5625 (9)	0·5625 (4)
	y	0·2348 (8)	0·2343 (4)	0·2345 (8)	0·2335 (3)
	z	[0]	[0]	[0]	[0]
	$\bar{B}$	3·7 (1)	3·27 (6)	3·34	2·25 (5)
V	x	0·3680 (7)	0·3655 (3)	0·3665 (8)	0·3651 (3)
	y	0·0399 (7)	0·0391 (4)	0·0390 (8)	0·0386 (4)
	z	[0]	[0]	[0]	[0]
	$\bar{B}$	2·9 (1)	3·19 (7)	3·34	2·51 (6)
R_{F^2} (%)		53·42	12·78	16·21	14·21
R_{wp} (%)		4·18	2·09	2·19	5·46
R_{exp} (%)		1·63	1·63	1·59	3·83

* Includes absorption and extinction corrections.

positional parameters are *consistently independent of the space group used for the refinement.* In particular, the values of those positional parameters which are required to have special values in the centrosymmetric space group $P4_2/mnm$ (No. 136) refine to values which are very close to these special values when the noncentrosymmetric space groups are used. This observation confirms the supposition of Donohue (1974) that the space group of β-uranium is the centrosymmetric $P4_2/mnm$ (No. 136).

The values of the R factors obtained for each space group (Table 3) are nearly the same but show a distinct trend R (No. 102) < R (No. 118) < R (No. 136). Since the number of observations in these time-of-flight experiments is much larger than the number of refined variables, these differences are significant in a strictly statistical sense. One must, however, take seriously the cautionary findings of Baur & Tillmans (1986) and of Marsh (1986) who have shown how the application of the usual statistical tests to nearly centrosymmetric structures can lead to erroneous conclusions, and we prefer not to rely on these tests in the case of β-uranium. Instead, we base our conclusions on the refined positional parameters themselves. In addition, the values of the anisotropic thermal parameters obtained in space group No. 136 which are given in Table 4 show very little anisotropy, further supporting the finding of centrosymmetry. In the absence of convincing evidence to the contrary, the structure of β-uranium is centrosymmetric.

So far, we have discussed the results obtained for powdered β-uranium by the application of the Fourier filtering technique to the powder data. It turns out that nearly the same refined positional parameters are obtained from the unfiltered powder data and for the polycrystalline rod data, as shown in Table 5. As expected, considerable variation of the refined values of

the thermal parameters is observed, and the effect of absorption and extinction corrections for the polycrystalline rod data is clearly evident in the lower thermal factors obtained in this case. These findings indicate that the absolute accuracy of the thermal factors of Fig. 5(*a*) and of Table 5 is not necessarily very good. The overall trends with regard to temperature and anisotropy may, however, be taken seriously.

Discussion of the structure

The structure of β-uranium is shown in Fig. 6, which is a composite of Holden's (1958) representation of the β-uranium structure and of Pearson's (1972) representation of the σ-phase. The centrosymmetry of the β-uranium structure which has been demonstrated by our experiment means that a *planar* configuration of the I, II, IV and V atoms which comprise the *B* and *C* layers is required by symmetry. Within the layers, the pseudohexagonal arrangement is not symmetry determined, but rather shows the influence of close packing on the atomic coordinates. The *A* layers, which are not closely packed, show a small (but significant) puckering. The structure of β-uranium is thus virtually identical to that of the σ-phase determined by Bergman & Shoemaker (1954). One consequence of the puckering is shown in the bond-length histogram of Fig. 7: the very short III–III bond of 2·78 Å. The puckering itself may be viewed as a Peierls distortion (Peierls, 1955) of

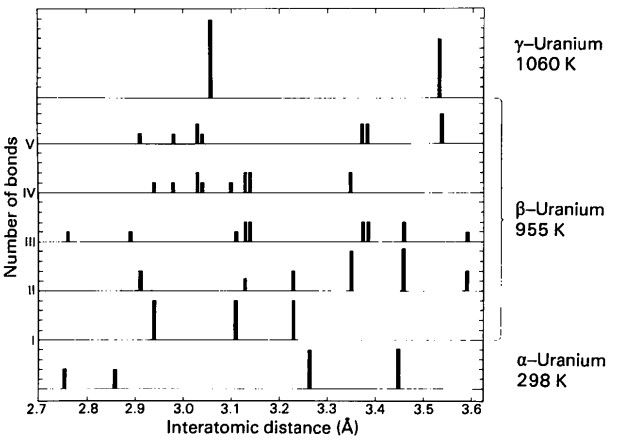

Fig. 7. Spectra of interatomic distances of a U atom, from the present results, in the three phases. Heights of the lines are proportional to the number of neighbours, the shortest line corresponding to one neighbour. Note: the shortest distance found in γ-uranium (3·06 Å) was incorrectly reported by Donohue (1974) as ~2·8 Å.

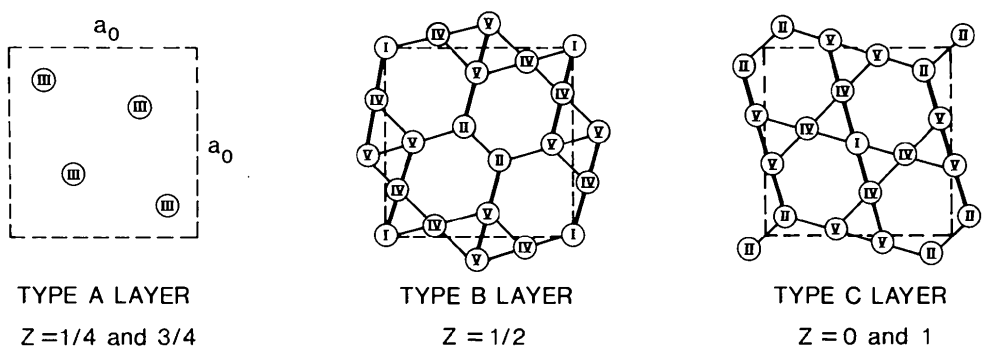

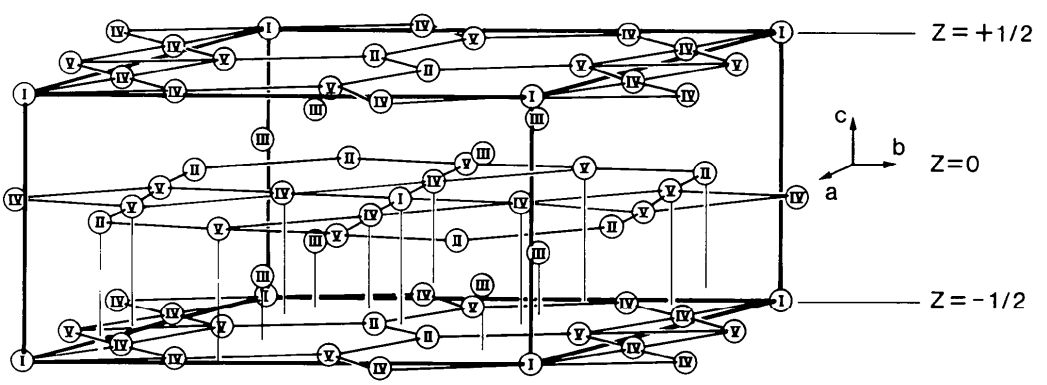

Fig. 6. Structure of β-uranium. Symbols refer to atoms identified in Tables 2 and 3.

the chains of III atoms running along the c axis, giving rise to alternating bonds of 2·78 and 2·89 Å. Except for a shortening of the shortest bond, the bond-length histogram of Fig. 7 is very similar to that given by Donohue (1974). The exception arises because Donohue chose the value $z = \frac{3}{4}$ for atom III, giving two bonds of 2·83 Å along the c axis. Our experiment proves that there are two short bond lengths.

Conclusion and summary

The principal result of our investigation is the demonstration that the β-phase of uranium has the centrosymmetric space group $P4_2/mnm$. The previous controversies (Donohue, 1974) are thereby resolved. The choice of space group depends mainly, although not completely, on the determination of certain z coordinates. For these investigations we have used neutrons (for which the absorption is very small) with a high-resolution diffractometer and the Rietveld profile method to increase the accuracy of the refined parameters. A powder sample was used to minimize the effects of grain growth and texture, and the background from the fused silica container was effectively removed (Richardson & Faber, 1986). All these methods are advances over those used in the original X-ray studies performed prior to 1970, and some confidence may be placed in the new results. Unfortunately, we still do not know why the structure of β-uranium is as complicated as it is, and the reasons for this complexity of structure remain one of the major unsolved problems in the crystal chemistry and physics of the actinide elements.

We wish to thank J. Faber Jr, R. L. Hitterman, F. J. Rotella and A. Severing for much advice and experimental assistance, and we are especially grateful to D. Wozniak for his help with the construction and calibration of the furnaces. Both ANL and LANL are supported by the US Department of Energy. IPNS is operated by the Basic Energy Sciences Division of USDOE as a National User Facility.

References

ARAI, M. (1984). IPNS Note 27. Argonne National Laboratory, Argonne, USA.

BARRETT, C. S., MUELLER, M. H. & HITTERMAN, R. L. (1963). *Phys. Rev.* **129**, 625–629.

BAUR, W. H. & TILLMANS, E. (1986). *Acta Cryst.* B**42**, 95–111.

BERGMAN, G. & SHOEMAKER, D. P. (1954). *Acta Cryst.* **7**, 857–865.

BROOKS, M. S. S., JOHANSSON, B. & SKRIVER, H. K. (1984). In *Handbook of the Physics and Chemistry of the Actinides*, Vol. 1, edited by A. J. FREEMAN & G. H. LANDER, p. 153 *et seq.* Amsterdam: North-Holland.

CHIOTTI, P., KLEPFER, H. H. & WHITE, R. W. (1959). *Trans. Am. Soc. Met.* **51**, 772–778.

DONOHUE, J. (1974). *The Structures of the Elements*, pp. 134–148. New York: John Wiley.

DONOHUE, J. & EINSPAHR, M. (1971). *Acta Cryst.* B**27**, 1740–1743.

DUWEZ, P. (1953). *J. Appl. Phys.* **24**, 152–154.

HOLDEN, A. N. (1958). *Physical Metallurgy of Uranium*, pp. 30–32. Reading, Massachusetts: Addison-Wesley.

JORGENSEN, J. D. & FABER, J. JR (1982). In *Proceedings of ICANS VI*, Report 82-80, edited by J. M. CARPENTER, pp. 105–112. Argonne National Laboratory, Argonne, USA.

JORGENSEN, J. D. & ROTELLA, F. J. (1982). *J. Appl. Cryst.* **15**, 27–32.

LANDER, G. H. & MUELLER, M. H. (1970). *Acta Cryst.* B**26**, 129–136.

MARSH, R. E. (1986). *Acta Cryst.* B**42**, 193–198.

MUELLER, M. H., HITTERMAN, R. L. & KNOTT, H. W. (1962). *Acta Cryst.* **15**, 421–422.

PEARSON, W. B. (1972). *The Crystal Chemistry and Physics of Metals and Alloys*, p. 675. New York: Wiley–Interscience.

PEIERLS, R. (1955). *Quantum Theory of Solids*, pp. 108–112. Oxford Univ. Press.

RICHARDSON, J. W. JR & FABER, J. JR (1986). In *Advances in X-ray Analysis*, edited by C. S. BARRETT, J. B. COHEN, J. FABER JR, R. JENKINS, D. E. LEYDEN, J. C. RUSS & P. K. PREDECKI, Vol. 29, pp. 143–152. New York: Plenum Press.

RIETVELD, H. M. (1969). *J. Appl. Cryst.* **2**, 65–69.

SMITH, H. G. & LANDER, G. H. (1984). *Phys. Rev. B*, **30**, 5407–5415.

VON DREELE, R. B., JORGENSEN, J. D. & WINDSOR, C. G. (1982). *J. Appl. Cryst.* **15**, 581–589.

Acta Cryst. (1988). B**44**, 96–101

Electron Density in Non-Ideal Metal Complexes. IV. Hexaaquametal(II) Ammonium Sulfates

BY E. N. MASLEN, S. C. RIDOUT AND K. J. WATSON

Department of Physics, University of Western Australia, Nedlands, Western Australia 6009, *Australia*

(*Received* 7 *February* 1987; *accepted* 29 *October* 1987)

Abstract

The electron-density distributions in $(NH_4)_2M^{II}(SO_4)_2 \cdot 6H_2O$, with M = Mg and Ni are compared. Both magnesium and nickel densities show approximate 4*mmm* symmetry, consistent with the geometries of the structures. The distributions near the metal atoms are similar, except for differences which can be understood in terms of the d electrons in the nickel structure. For the shortest nickel–oxygen bond there is a deep

0108-7681/88/020096-06$03.00